

***BASIC KNOWLEDGE ON THE HIGH-RESOLUTION
ASTRO-SPECTROSCOPY
AND THE REQUIRED INSTRUMENTATION***

Dimiter KOLEV

NAO “Rozhen”

dzkolev@abv.bg

Presented on the First School on Astro-spectroscopy,

NAO “Rozhen”, 21-27 October 2007

Bulgaria

1. ASTROSPECTROSCOPY AND ITS ROLE FOR THE ASTROPHYSICS

1.1. Instrumentation and cost of the astrophysical observation

The high-resolution astro-spectroscopy has begun since the mid-30-es years of the 20th century. Then the big diffraction spectrograph in the coude-focus of the 2.5m Mt Wilson telescope came into operation. Since that time the evolution of the astro-spectroscopy gives us an excellent example for the art of compromise following often mutually excluded conditions and requirements: vanishing-low energetic fluxes; more and more severe claims to the spectral, time and space resolution; to the photometric and positional accuracy, etc. And all this depends also on the technical and technological achievements and on some economical reasons, as far as the astrophysical instrumentation is among the most expensive scientific tools!

Example: 2m RCC at NAO “Rozhen” costs ~5 M\$ (70-es years of 20th century) and the whole Observatory – ca. 10 M\$ (in the same time, the ESO-investment in VLT – Very Large Telescope, 4 x 8.2m – was ca. 1 G\$). The annual subsidy of NAO is around 100-120 K\$ and the real observing time – about 1000 hours/year. Considering a life-time of 100 years for the telescope and constant subsidy, we obtain a *cost of one observing hour* ~150 \$ or ~2.5 \$/min. For comparison: the telescopes of class 4-6 m spend ~15-25 \$/min, VLT – 4x60 \$/min; one observing night on Kecks costs 47000 \$!

What we can obtain for these “prices” from the observations? In fact, every observation of an astrophysical object is spectral one, as far as at least the detectors (including the human eye) are spectral-selective. The difference lies mainly in *the band of transparency* $\Delta\lambda$ and in *the resolving power* R:

$$R = \lambda/\delta\lambda, \quad (1.1)$$

where $\delta\lambda$ is the spectral resolution, i.e., *the registered by one detector’s element (pixel) spectral interval*.

Hence, the *resolving power* R is a measure of the possibility to register with given spectrograph close wavelengths simultaneously. This basic spectral characteristic does not have a physical mean, but is simply a handy scalar parameter. For *observations with eye* when the retina detects radiation in wide spectral interval of ~2000 Å centred on 5500Å, R~3. The photoelectric photometry with *one-channel* photometer is the same, despite more narrow filters and R~10-20.

The very spectral observation means to observe given interval wavelengths $\Delta\lambda$ on n elements of the detector, i.e., one element “sees” interval

$$\delta\lambda = \Delta\lambda/n \quad (1.2)$$

and hence the resolving power will be $R=n \lambda/\Delta\lambda$.

Example: a photometer at NAO after 10-sec integration gives a signal coded by 2-byte word; then the “price” of the information will be $p \approx 0.2$ \$/byte (2.5 \$/min*1/6 min / 2 byte = 0.2\$/B). Our high-resolution spectrograph for 10 min obtains a spectrum of 200 Å around 6500 Å, in $n=1000$ channels (pixels); the resolving power is $R=1000 \times 6500/200=32000$, and the “price” of 1 byte (considering 2-byte word) $10 \text{min} \times 2.5 \text{\$/min} / 1000/2 \approx 0.01 \text{\$/B}$. We see that the “spectral” byte is much more “cheaper” than the photometric one. The old photographic technology needed much more time and therefore the “price” of the spectrograms was much higher!

So, different kinds of astrophysical observations give different amount of “formal” information: from 1-2 byte (photometry) till hundreds Kb and Mb for high-resolution spectroscopy. Evidently, the *economic* costs of this information could be different by orders.

However, what about the scientific value of the different kinds (modes) of observation? Such a question is rather relative because it is evident that the different kinds of observations are complementary each to other giving the complex picture of the events. Let us to consider the two observational methods: *photometry* and *high-resolution spectroscopy*. Giving us only several numbers – the brightness in wide filters – the photometry is in the basis of any investigation! It has the most wide application, the deepest magnitude-limit and gives the most general relations, such as HR-diagram in the form “color-color”. In fact the photometry is an observational technology for investigation of the distribution of the energy in the continuum spectrum. It allows an absolute calibration. Here the element that separates the requested spectral interval (from hundred to several Å) is some kind of filters (glass, interference, etc.). Having deep limit and easily calibrated relations between the photometric indexes and the physical parameters (temperatures, gravitation, magnetic

fields, polarization, chemical abundance, etc.) the stellar photometry is on the beginning of the study of any unknown object while for the weakest ones it is the only applicable method!

Close to the photometry is the *spectro-photometry*. In fact it is realised by one-channel photometer which scans the spectrum by “portions” (usually about 50 Å). Here the filtering element is a coarse diffraction grating with low resolving power ($R \sim 100-200$) and the spectral interval is separated by a slit before the photo-cathode of the multiplier. This method also studies the stellar continuum, it is a subject of calibration procedures and is extremely valuable for studying the distribution of the energy (e.g., needed for modeling the stellar atmospheres).

The electromagnetic optical spectrum can be divided to the next intervals:

- far (vacuum) ultraviolet (UV) – from 10 to 1850 Å;
- near-UV – 1850 - 4000 Å;
- visual region – 400 - 7000 Å;
- near infrared (NIR) – 0.7 μ (7000 Å) - 2.5 μ ;
- mid-IR – 2.5 μ - 50 μ ;
- far-IR – 50 μ - 1000 μ (1 mm).

The astro-spectroscopy begins with the registration of the spectrum in many channels and can be divided (rather provisory) by its resolving power R . Somebody considers observations with $R \leq 20000$ as having “low resolution”, with $20000 \leq 60000$ – as “middle resolution”, about $R=100000$ – as “high resolution” and with $R > 120000$ – as “super-high” resolution. These values of R correspond for $\lambda = 5000$ Å to a spectral range per one pixel as follows: ≥ 0.25 Å for the low-resolution mode; 0.25-0.08 Å for the middle R , about 0.05 Å for the high-resolution mode and ≤ 0.05 for the super-high resolution.

It must be noted that during the “photographic” era as high-dispersion ones were considered observations with *reversed linear dispersion* (see below) $\Delta\lambda \leq 10$ Å/mm. Assuming mean size of the resolving element $p=20$ microns, we obtain for the resolving power a value $R \geq 25000$. The replacing of the photo-emulsion with solid-state detectors, which have dozens of times higher sensitivity and allow working with earlier unprecedented SNR, has changed the ranging of the notion for the resolving power.

Example: investigations having $S/N \sim 300$ and $R \sim 100000$ on Ila-O or IIIa-J astro-emulsions with 1-2 m telescopes were possible only for Sirius, but they have need at least 30 min exposure and widening of the spectrum’ strip to 5-6 mm on the emulsion! In the same time illuminating the whole slit-length (10 mm) of our coude with Sirius, we obtain by LN₂-cooled CCD spectrum of $S/N \sim 1000$ for only 20-30 sec exposition! The spectrum has a height of 1.75 mm (76 pxl) on the detector.

The spectral resolving power degrades by many reasons. Besides the purely physical ones (diffraction) the others are mainly technical: the finite size of the entrance slit; the optical aberrations, defects and adjustment errors; the characteristics of the detector (e.g., the “2-pxl” rule about the final size of the resolving element for CCDs). In the same time, enhancing R the economic price of the spectral device also enhances (remaining, however, a relatively small part ($\sim 10\%$) of the telescope’ price. So, the complete price of the coude-spectrograph of the 2m telescope at Rozhen is $\sim \$500000$ and the price of a modern echelle-spectrograph is about $\$150000$.

But why the astrophysicists strive for greater resolving power? Evidently, because they need more and more information about the objects they study. As many as independent channels receive simultaneously information, so many will be its amount. The high- and super-high resolution spectroscopy is *the only* observational method to obtain a *detail* picture of the light-intensity distribution along the wavelengths. **All branches of astrophysics need high-accuracy and with high spectral resolution observations.**

1.2. Information obtained from the astrophysical objects’ radiation

The celestial bodies emit themselves or reflect other radiation and just because of that they are visible. Every energetic flux has its own distribution along the radiation frequencies. In the ideal case it can be the Planck distribution of an equilibrium radiation with given temperature T . Among the stars closer to the Planck-distribution are the O- and early B-stars that have effective temperatures $T_e \geq 20000$ K (by the way, the term “effective temperature” is defined just by the Planck law – it is the temperature of the black body which total radiation is equal to the total flux from the star). One can note, however, that all the

“temperatures” considered here and below characterise only the outermost stellar layers calling “stellar atmosphere”.

As colder is the star, as farther is their radiation distribution from the Planck’s one. The main reason for this is the blanketing effect – the absorption of the light in numerous spectral lines of different neutral and of low ionization atoms. Let’s consider an ordinary MS-star of spectral class A ($T_e \sim 9000 - 10000$ K). Such a star has a compact atmosphere ($H \sim 1000$ km that is only 0.1-0.03% of its radius). The local temperature drops toward the surface layers. The conventional boundary, above that the atmosphere begins, we call “photosphere” and it can be in some way to be compared by the Earth’s surface. Of course, in the star we have not so sharp division, on both “sides” of this boundary there is plasma and the only criterion is the *optical depth* τ – a characteristic for the light intensity decreasing when the radiation passes given medium. We have $\tau = 1$ when the intensity drops e -times ($1/e = 0.37$). The stellar atmospheres theory gives a value $\tau = 2/3$ (it means two-times decreasing in intensity) for the boundary from which the continuum spectrum is emitted. If cooler layer lies above the photosphere, it will absorb energy from the passing continuum flux. Besides the general absorption there exist a selective one in the energy levels’ frequencies of the atoms and ions composing the atmosphere. The resulting picture is typical stellar absorption spectrum (Fig.1).

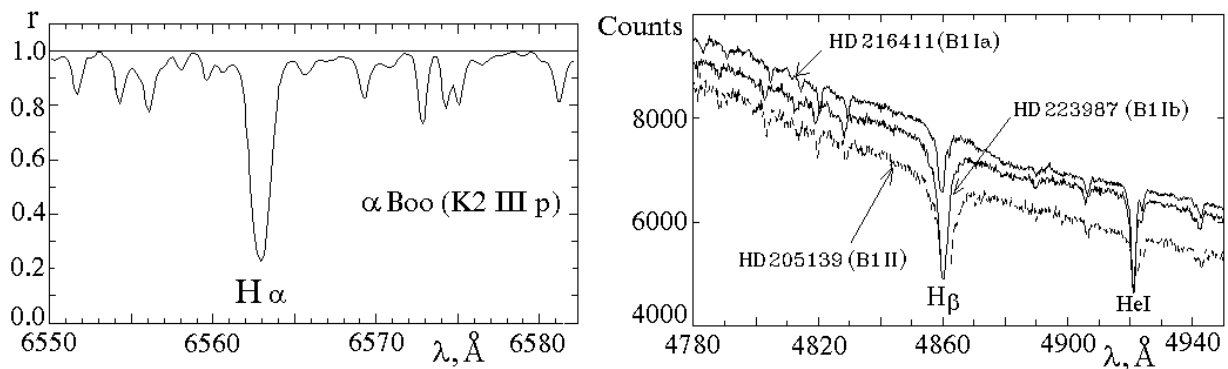


Figure 1. Spectra around the hydrogen line $H\alpha$ of the star α Boo ($V = 0.16^m$, K2III) (left panel, normalized) and around $H\beta$ in B-supergiants of different luminosity class (right panel, raw data). Note the different widening of the hydrogen lines due to different pressure in the atmospheres of different stars!

When the stellar atmosphere is more prolonged, as it is in the giant, supergiants and some hot B-stars, it can be possible to observe spectral lines in emission. It superpose the unavoidable absorption line giving different kinds of so called “P-Cyg” profile – Fig.2.

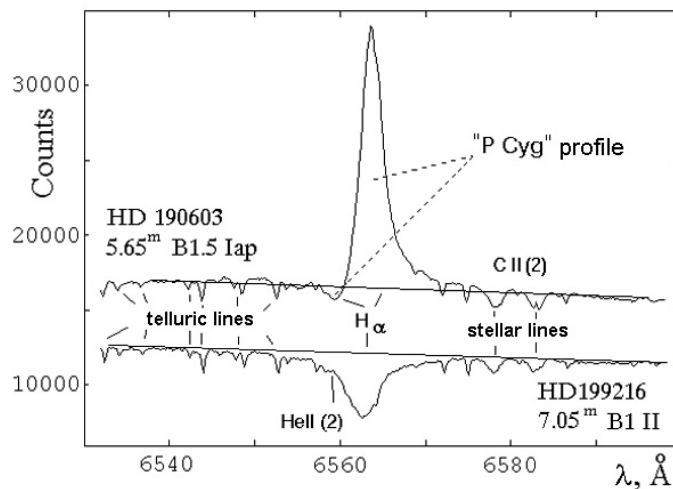


Figure 2. “P-Cyg” type profile of $H\alpha$ in the star HD190603 ($V = 5.6^m$, Sp B0-B1.5 Ia, “a shell star”). For comparison the spectrum of the “normal” B-star HD 199216 ($V = 7.05^m$, B1II) is also presented. Also well seen are the telluric absorption lines arising in the earth atmosphere due to the water molecules absorption.

The shape of the hydrogen lines is sensitive to the gas pressure and, therefore, to the gravitational potential in the atmosphere. These lines can help us to derive the luminosity class of the star (see Fig.1, right).

Due to the Doppler-effect the frequencies in the spectral line arising in moving volume shifted and deformed the line-shape. So, we can study the different star motions looking at the line shape!

The “strength” (the intensity) of the lines gives us information (both qualitative and quantitative) about the chemical abundance of the atmosphere. It is possible also, using the spectral lines, to investigate the magnetic fields, if they present in the atmosphere.

1.3. General scheme of the astrophysical investigation

The based on earth ground observations astrophysical investigation is carried out following the next general scheme (Fig. 3).

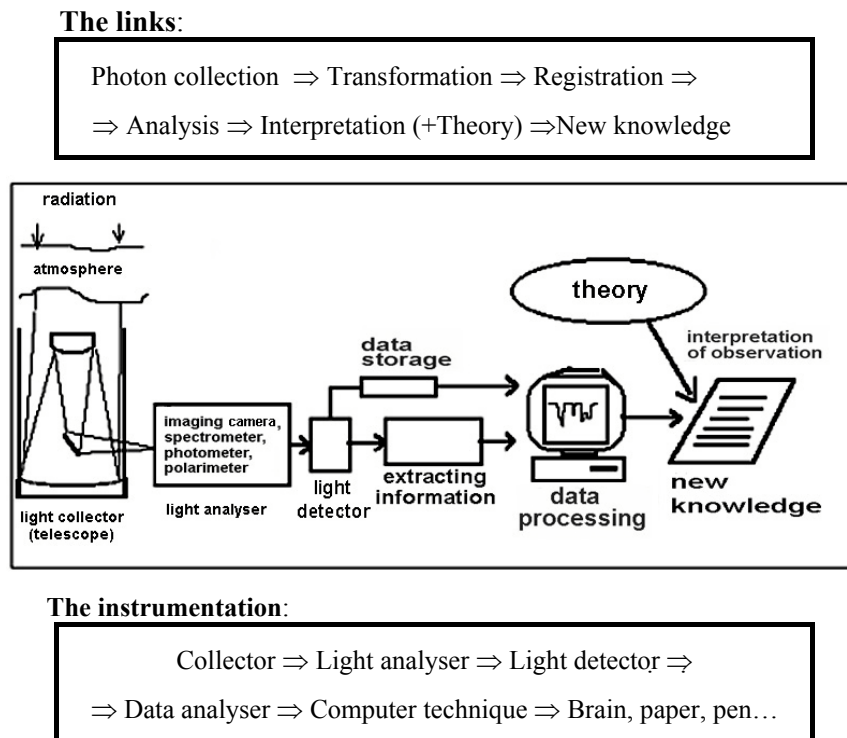


Figure 3. General scheme of the astrophysical investigation

The elements in this scheme have the following function:

The collector (telescope) has two-fold role:

- 1) **to collect** as much as possible energetic flux from sky sources in given solid angle;
- 2) **to project** the sky picture onto the focal plane with suitable for the scientific aim linear scale.

The light-analyser is a special device that can be placed as pre-focal (before the main mirror: objective prism or grating, stellar interferometer, etc.), as focal (e.g., direct imaging camera, photometer and/or polarimeter, spectrometer, etc.).

The light-detector is a physical medium that, under the radiation, changes its condition on exactly known and stable law for any length of time or forever.

Up to the end of 80-es of 20th century the most spreaded detector was the **photoemulsion**. There are countless glass plates in the observational archives all around the world and the information on most of them still are unused! Despite numerous advantages (panoramic, big storage capacity, stable, etc.) the most important shortcomings of the emulsions (non regularity, complex processing, low DQE (Detective Quantum Efficiency), low SNR (Signal-to-Noise-Ratio), non-linear response on the incoming light, complex

and expensive devices for deriving information, etc.) judged their disappearance when the new solid-state detectors were developed and matured.

The modern solid-state detectors, typical representative of them being CCD, have remarkable advantages in comparison to the emulsion:

- great peak DQE (up to >90%);
- high linearity of the response
- great dynamic range (>100000);
- high SNR per pixel (depending of the integer-value of the ADC; so, 16-bit ADC fills the pixel with 65500 ADU, i.e., SNR=250 per pixel;
- direct numerical output;
- equal geometry (strong spatial homogeneity!);
- easy for maintenance (especially for the CCDs with Peltier-cooling);
- easy control and summation of the frames, improving the noise characteristics.

The present disadvantages of the CCDs are:

- still smaller linear dimensions than that of the photoplates. So, the biggest single chip produced by DALSA (2006) has 111Mpxl and size of ~100x100 mm that is 25 times less than the area of the biggest astroplate being in use. Combining several CCD chips in a mosaic it is possible to cover area quite comparable with such a huge astroplate, but the price of such a device reaches M\$-levels.

- existence of parasitic signal sources, especially the cosmic spikes; they often limited the reasonable exposure time to less than 30 minutes!

- more complex and expensive maintenance of the LN2-cooled CCDs.

The information-analyser is of need mainly when photo-plates are considered; it is a sophisticated device (densitometer, comparator, etc.) which scans and digitises the “hidden” in the emulsion information.

Of essential importance is to recognise that in *every* link of the considered process (including the interpretation and the theory steps) *parasitic noises* are involved. They deform and deteriorate the signal and the information and decrease the SNR. Some of these noise-sources are:

- **the earth atmosphere** – the turbulence deforms the wave-front causing the so called “turbulent disk” in the focal plane of the astronomical telescopes. The angular dimension of this disk is hundred times greater than the diffraction image produced by the earth-based telescopes with aperture greater than, say 1-m. This decreases the *light-concentration* in the focal plane (degrades the *frequency-contrast-function*). The atmosphere degrades also the signal *amplitude* and makes it spectral selective (!); it disperses the “white” light (especially on great zenith distances!), etc.;

- **the aberrations** of the telescope and spectroscopy optics;

- **the light-analyser** itself (photometer, spectrograph, filter, polarimeter, etc.) has its own instrumental noise-sources that degrade the signal. Here we can enumerate the electronic, thermal, and other noises; the scattered light; the mechanical deformations and aberrations, etc.

- **the detector** is also noisy: the photo-emulsion scatters the light and the CCD camera has many noise-sources, such as the photon, the thermal, the reading noises, the interference fringes, etc.

- **the information-analyser** also is noisy due to its own optics and electronics;

- **the info-processing** – e.g., every mathematical filtering losses info; the different software packages can be based even on different philosophy of the data processing, etc. The theory also is not insured against wrong conclusions, interpretations and “interventions” in the astrophysical investigations.

So that, in order to complete successfully the astrophysical investigation based on real observations, numerous factors influenced the obtaining and the processing of the raw data must be taken into account.

2. THE BASIS OF THE ASTRO-SPECTROSCOPY

2.1. Physical processes dispersed the light

We shall begin with reminder some basic for the wave-optics conceptions:

- **dispersion** (from the Latin *dispero* = break up, intersperse among, intersperse between; distribute) we call in general the way by which given physical system react to the outer influence. Considering the light-wave propagation we distinguish **the material dispersion** (that characterizes the dependence of the refracting coefficient from the wavelength) and **the device dispersion** – the ability of the given physical system to separate by some way (spatial or temporal) the light-waves of different frequencies;

- **monochromatic** is an infinite sinus-wave with permanent frequency (wavelength); it has strongly definite phase in given spatial point;

- **coherent** are waves with permanent phase-difference; all monochromatic waves with equal frequencies are monochromatic;

- **incoherent** are waves with different phase-difference; it can be as waves with different λ , as also waves with equal λ , but consisted of independent “packets” with random phases in the beginning and in the end of every packet.

- **interference** is the phenomenon of decreasing or increasing of the *amplitude* when several coherent waves overlap. By summing flat coherent waves with phase difference $\Delta\omega=0$ their amplitudes are summed; if the $\Delta\omega=\pi$ then the amplitudes are subtracted. The intensity of the resulting wave is equal to the square of the amplitude. If incoherent waves are summing we observe only an increase of the intensity – such waves do not interfere!

- **diffraction** in a broad sense we call all phenomena manifesting a declination from the geometric optics laws when the wave is propagated during given medium. Due to the diffraction the light can be found even in the region of the geometric shadow; the waves can go round physical obstacles, they can “envelope” surfaces, etc.

A beam of “white” light collected by the telescope mirror consists of mix of waves with different wavelengths and phases (i.e., **incoherent**). They are propagated in one and the same direction and in one and the same geometric path. Hence, *the different frequencies are not spatially separated!* If such a beam meets a physical medium that is able to separate spatially the particular waves we can register the *frequency-spectrum* of this radiation. In the astrophysics mainly three methods for spatial separation of frequencies are used (Fig. 4): *refraction* of the light on the boundary of two media; *diffraction* of the light on number of openings; *multi-beam interference* due to multiple reflection.

Technically these methods are realised respectively by the following dispersing optical systems: *prisms*, *diffraction gratings* and *interferometers* of different kind. *All these devices work properly in a parallel beam.*

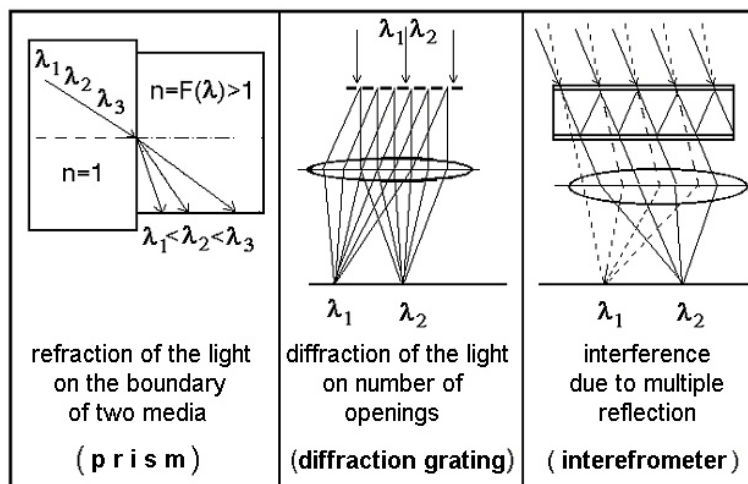


Figure 4. Optical phenomena of light dispersion

It can be noted that, especially for the IR-spectral range, some other physical principles can be used in order to separate different spectral intervals of interest: Fourier-spectrometer, Spectrometer with Interferential Selective Amplitude Modulation (SISAM), or Bragg fiber gratings (a fiber with core of variable refractive coefficient). They could be used also in astronomy.

2.2. Principal design of a high-resolution astro-spectrometer

The principal structure of the “classic” astro-spectrometer (Fig. 5, left) and that of the coude-spectrograph of the 2-m telescope at NAO “Rozhen” (Fig.5, right) includes the next elements:

- **entrance slit** – two sharp knives from inox-steel. Their edges form constant in shape and position light-source for illumination of the collimator during the exposure. The knives-plane is slightly sloped (for our coude-spectrograph on $\sim 12^\circ$) in relation to the optical axis and the polished surface of the slit reflects a part of the star image allowing control of the slit-illumination during the exposure. The star image is focused on the slit;

- **collimator** – it transforms the conical beam to parallel one and directed it to the disperser;

- **disperser** – prism or grating;

- **camera** – optical device to project and register the spectrum;

- **detector**;

- **calibration systems** – for wavelength, flat-field or photometric calibrations; filters, etc.

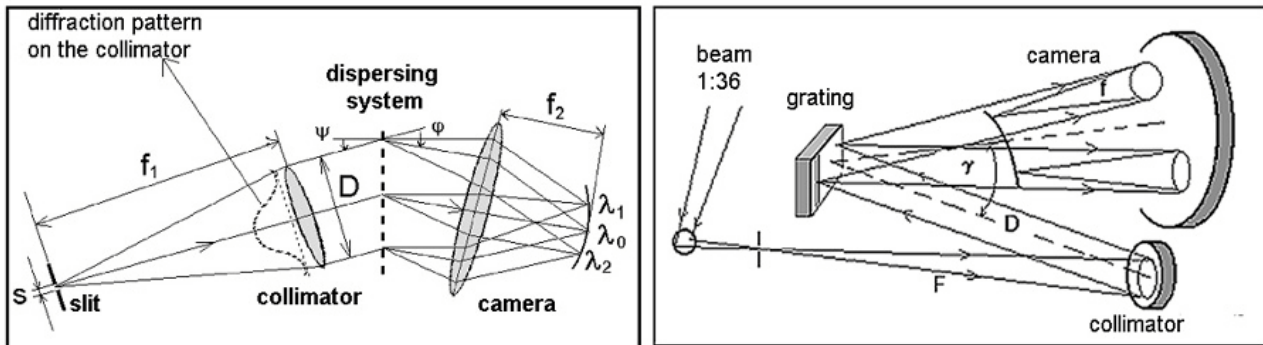


Figure 5. Structure of a spectrometer (left panel) and a scheme of the coude-spectrograph in NAO “Rozhen” (right panel)

2.3. Light-efficiency

Before more detail treatment of the spectral instruments lets to concentrate the attention on the very important for the slit-spectroscopy question about the light efficiency and light-losses. The slit is illuminated by focused light beam collected by the main mirror. The light losses here sometimes are discouragingly great.

Example: light-losses in the coude-spectrograph of the 2-m RCC telescope at NAO “Rozhen”:

1. Loss due to reflections – every mirror-reflection from Al-surface suffers loss in intensity from $\sim 10\%$ (for fresh Al-layer) until 20-25% for old one. Our coude-focus is formed after 5 reflections: main and secondary mirrors (angle of incidence $\sim 90^\circ$), two 45° -reflections from the flat mirrors in the declination axis of the telescope and one flat reflection under $\sim 70^\circ$ from the deflecting mirror before the slit. Assuming reflection coefficient of 0.8 we obtain that only $\sim 33\%$ (0.8^5) of the collected light reaches the entrance slit!

In the spectrograph itself we have: 3 mirror reflections (collimator, camera mirror and deflecting flat mirror before the CCD-camera) and one spectral selective reflection from the grating. Assuming the same coefficient of 0.8, we finally obtain the efficiency due to the reflection-loss to be only 0.17. That means loss of 83% !

2. Geometrical losses – they are of several kinds:

a) – **slit-loss**: the scale on the slit is $l/\alpha = F \sin 1''$ [mm/"] and for our 2-m telescope with $F=72000$ mm we have a scale $72000/206265=0.35$ mm/" or ≈ 3 "/mm. As far as our seeing in coude often is just 2"-3" (~ 1 mm) and the working slit is 0.2-0.3 mm, the **slit-loss** of light reaches once again 70-80% !

b) – **shielding-loss** (vigneting): for some working angles the cross-section (an ellipse) of the collimated beam and the grating plane can overfill the grating length and for our gratings it can cause $\sim 10\%$ loss; similar losses can cause the shielding by the groove shape for great angles of incidence.

c) – **vigneting-loss on the slit** due to de-focussing of the secondary mirror: as can be seen in Fig. 6 if the instant focus do not coincide with the slit-plane, it is possible a part of the collimator can be shadowed. Besides the light loss such a situation produces also positional errors when project the spectral lines on the detector plane!

This situation is especially important for the coude-focus; due to the very long focal distance the position of the instant focus strongly depends on the atmosphere conditions and the zenith distance to the object. The de-focusing ΔF along the axis before the slit is 80(!) times greater than the axial shift of the secondary mirror ΔS .

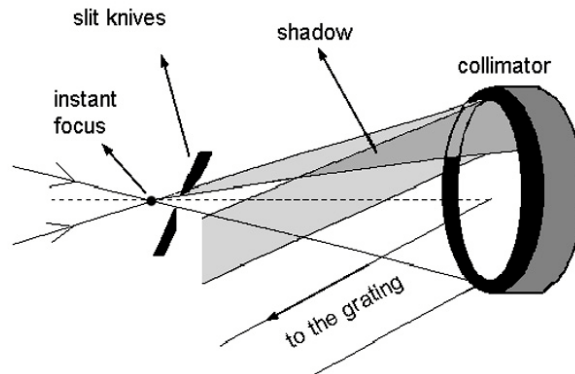


Figure 6. Shadowing by the slit edge due to de-focused star image

d) – *light-loss due to incorrect position and guiding of the star image on the slit:* the atmosphere plays a role of a prism for significant zenith distances. This phenomenon is known as “atmospheric dispersion”. Additionally the coude-field of view *rotates* with the time, so that the *position* of the star image on the slit changes during the exposure. So, if we expose certain spectral range, say, “red” and on the slit the “blue” one is placed, the light-loss can be great or even we will register nothing!

The angular dimension (in angular seconds) of the atmospheric spectrum, expressed by the difference in the *zenith distance* of the image in the boundary wavelengths (in microns) is:

$$\Delta z \approx 0.335 [1/(\lambda_1)^2 - 1/(\lambda_2)^2] \text{tg}z.$$

For example, observing an equatorial star in the meridian from NAO “Rozhen” it will have $z = \varphi \approx 42^\circ$ and the “visible” spectrum from 4000Å (0.4μ) till 8000Å (0.8μ) will be extended in 1.4" with linear size of 0.5 mm in the coude-focus. It is almost twice greater than the working slit width. At a whole, the “visible” atmospheric spectrum depends on z as $\Delta z \approx 1.5'' \text{tg}z$ and for zenith distance $z = 70^\circ$ its angular size of 4" corresponds to a length of 1.5 mm while the slit is only 0.3 mm wide! Hence, if we need a spectrum around 8000Å but during the exposure the “blue” end is on the slit, we really will obtain nothing!

3. Light-loss due to the detector: the peak DQE of the present CCDs is far above 80% but in the end of their working spectral range it can drop drastically (see Fig. 7). Assuming 70% as an average value for the most spectral ranges of interest, we see another 30% loss in light!

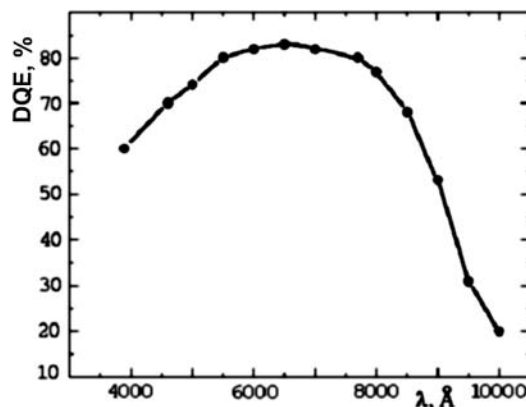


Figure 7. DQE of the SITe 1024 CCD-chip

At a whole, the total light-efficiency of a “classic” coude-spectrograph like our in NAO “Rozhen” in the best case will be a few percents (~3%)! In the “photographic” era the situation was much worse – the DQE of the best astro-emulsions did not exceed 4%, so the total efficiency was only ~0.1% ! That is why a star of magnitude $V = 6^m$ needed 1-2 hour exposure time and the resulted SNR in the continuum was only 30-40.

2.4. The spectrograph optics

2.4.1. General construction and concordance of the spectrograph

As it was already noted, the art of the astro-spectroscopy is an art of compromises. Why the astrophysicists become reconciled with enormous light-losses in the stellar slit spectroscopy? Why we can not work, say, with *wider* slit, for example?

The leading consideration here is the wish to work with high spectral resolution. But before to examine in detail the spectrographs' schemes we shall discuss the very important for the astrophysics matter of the concordance of the parameters of the light-collector (the telescope) and the light-analyzer (the spectrometer itself). It is obviously an *outer* for the spectral device co-ordination. The idea is clear – as can be seen in Fig.8 the practical rule will be: the spectrometer's collimator must have the same *relative aperture* (*focal ratio* or *f-ratio*) as the telescope optics for the given focus. If the diameter of the collimator is smaller we evidently will loss light due to overfilling of the collimator. The opposite case of an under-filled collimator do not affect the observations but unduly makes the optics more expensive.

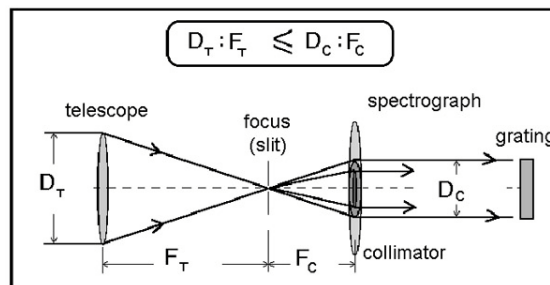


Figure 8. Concordance between the telescope and the spectrograph

Example: what must be the parameters of a collimator for the coude-spectrograph of the 2-m RCC telescope at NAO “Rozhen” if the *f-ratio* of the coude-focus is 1:36 and the gratings have a grooves' height of 300 mm?

The collimated beam must fill exactly the grating hence the collimator's diameter must be at least 300 mm. From the concordance rule it follows that the *f-ratio* of the collimator must be 1:36 and for $D=300$ mm we obtain a focal distance for the collimator $F_{coll}=300*36=10800$ mm.

Lets return to the general scheme of the spectrometer (Fig. 5). The slit is placed in the focus point of the collimator with aperture D . The collimated parallel beam of “white” light has the same diameter and reaches the dispersing system under angle of incidence ψ . The disperser separates the individual beams for every wavelength and directs them in different diffracting angles ϕ . The “fan” of monochromatic parallel beams (every one with its own, *different, but close to D* aperture!) is focused by the camera's objective and forms the spectrum of the incoming light on the detector's surface. *This picture actually is overlapping of countless (if the source has continual spectrum) or is a number of monochromatic images (for linear spectrum) of the slit opening.* If F_{coll} and F_{cam} are the focal distances of the collimator and the camera and s is the entrance slit' width then s' will be projected onto the detector as

$$s' = s \cdot g \cdot F_{cam} / F_{coll} ,$$

where $g = \cos\psi / \cos\phi$ is known as “*geometric magnification of the grating along the dispersion*”. For the classic astro-spectrographs $g \sim 1$ (for our coude-gratings we have $g \sim 1.0-1.1$)

The above adduced simple geometrical considerations lead us to the next concordance rule: that of the entrance slit' width and the size p of the sensor' pixel (Fig. 9).

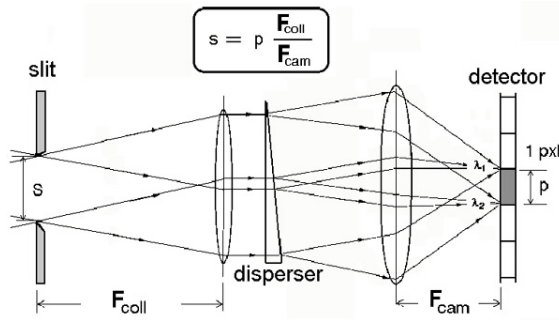


Figure 9. Concordance of the slit width and the detector pixel

As can be seen from Fig. 9, the optimal slit width that is projected exactly on one pixel will be

$$s_{opt} = (pg) \cdot (F_{coll}/F_{cam}) = pg b_s$$

The quantity $b_s = F_{coll}/F_{cam}$ can be named “slit-widening scale” and for the stellar spectrometers it plays an important role: as great is b_s , as more wide can be the entrance slit, improving the light-efficiency of the facility! Here we meet one more inconsistency characteristic for the astro-spectroscopy: the camera resolution depends evidently on the its focal length, i.e., the long-focal cameras are better in this sense, but it follows also proportionally longer collimator focal distance, if we wish to keep the light efficiency unchanged. The last requirement, however, raises the cost of the instrument, etc.

2.4.2. Diffraction grating and its equation

Let’s turn now to the physics of the light dispersion by a flat *diffraction grating* (DG). The reflecting DG is a structure consisting of many, usually equal in width, parallel strips, ruled (engraved) on *Al*-coated glass blank or produced by holographic method.

Here the realm of the wave-optics begins but for simplification we shall use also “geometrical” approaches and analogues. We shall illustrate the phenomenon in Fig. 10a by “transparent” grating but just the same conclusion and expressions take place also for the most frequently used reflective gratings.

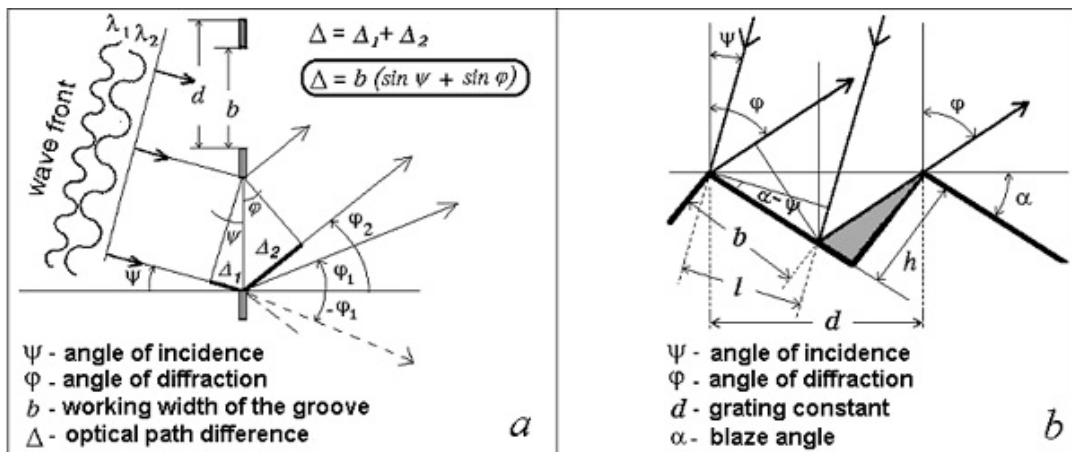


Figure 10. Principle scheme of a transparent diffraction grating (a) and blazed reflective phase grating (b)

The angles of incidence ψ and diffraction φ are read referring to the normal n to the main grating plane. They are both positive if are placed on one and the same side to the normal. The beams with different wavelength λ are diffracted under different angle and the longer waves the greater is the deviation (quite opposite to the case of refraction in a prism!). For given angles of incident ψ and diffraction φ the total difference in the

optical path Δ of the both endmost beams from **one** groove (or opening) for given wavelength λ (with its own angle of diffraction $\varphi=\varphi_\lambda!$) will be

$$\Delta = b(\sin\psi + \sin\varphi),$$

where b is the *actual* width of the groove. The condition for maximum intensity is

$$\Delta = b(\sin\psi + \sin\varphi) = k\lambda, \quad k=0, \pm 1, \pm 2 \dots$$

The diffraction grating with length (base) of the ruled area B consists of finite number N grooves. So **one groove** occupies space d :

$$d = B/N.$$

The quantity d is called “grating constant” or “groove period”. The more widely used is the “grooves density” N_1 , given in *lines-per-mm* and equal to $1/d$. For the visible spectrum the most widely used gratings have lines-density from 300 to 1200 1/mm. The gratings used in the present astro-spectroscopy most often are reflective and “blazed”, i.e., they have groove strips *inclined* to the grating plane under angle α (“blaze angle”). This groove geometry allows the maximum light concentration in desired spectral order.

The geometry of the blazed grating is presented in Fig. 10b. The *actual* width b of the groove depends on λ by the diffraction angle φ and can be smaller than the nominal one (note the shadowed area on the figure) for some directions.

The distribution of the intensity I (Fig. 10) as a result of the combined contribution of all grooves, i.e., after the interference of the N beams in given direction (diffraction angle φ) is given by

$$I=(I_0/N^2). (\sin^2u/u^2). (\sin^2Nv/\sin^2v) = F_0(N). F_1(u). F_2(N, v).$$

F_0 is the normalization term. The function F_1 gives the *diffraction* of any separate groove and the argument is

$$u = \pi b(\sin\psi + \sin\varphi)/\lambda$$

while the function F_2 gives the *interference* of the N parallel beams and is decisive for the main grating characteristics and for the position of the maximum. Here the argument has similar look as for F_1 but instead of the working width b the grating constant d is used:

$$v = \pi d(\sin\psi + \sin\varphi)/\lambda$$

Obviously we shall have a zero-intensity when at least one of the two “angular-dependent” functions $F_1(u)$ and $F_2(N, v)$ becomes zero. The minimum-condition for $F_1(u)$ is:

$$u=k\pi, \quad \text{or}$$

$$k\lambda = b(\sin\psi + \sin\varphi), \quad k=1, 2, 3, \dots$$

Because of the small value of b (for groove density 600 – 1800 mm⁻¹ both b and d are of order of 1 μ) the minima due to $F_1(u)$ are extremely rear. It follows also from the great angular width of the diffraction function (see Fig. a). Conversely, the great number of the grooves in the grating (e.g., for our holographic grating with grooves area of 360 mm length and density of 1200 mm⁻¹, $N=432000$) determines the frequent appearance of minima of $F_2(N, v)$ (Fig. b). In fact between the main maxima $N-2$ secondary maxima are placed, but, being numerous, they practically are fully suppressed. The condition for minimum of $F_2(N, v)$ is

$$Nv = n\pi, \quad n \neq kN, \text{ i.e., } n \text{ to be non aliquot to } N.$$

If n is aliquot to N , then $v = k\pi$ and $F_2(N, v) = N^2$. Instead of minima, we shall have *main maxima* with the condition

$$d(\sin\psi + \sin\varphi) = k\lambda$$

This expression is known also as “diffraction grating equation”.

This expression shows that for given λ rays with wavelengths aliquot to λ diffracted and have a maximum in the same direction! So the DG produces multiple spectra that is why the quantity k is called a *spectral order*. From the grating equation immediately follows that $|\sin\psi + \sin\varphi| \leq 2$, so the working order of given grating can not exceed a value

$$k_{max} = 2d/\lambda .$$

Example: for a grating with density 1200 mm^{-1} the constant is $d=0.83 \mu$ and for wavelength $\lambda = 6500\text{\AA} = 0.65\mu$ we shall have the limit $k_{max} = 2*0.83/0.65 = 2.56$ or for this wavelength this grating works only in 1st and 2nd orders (see Fig. 11). For the blue-violet light with $\lambda = 0.4\mu$, $k_{max} = 4.16$ and the grating can work up to 4th order.

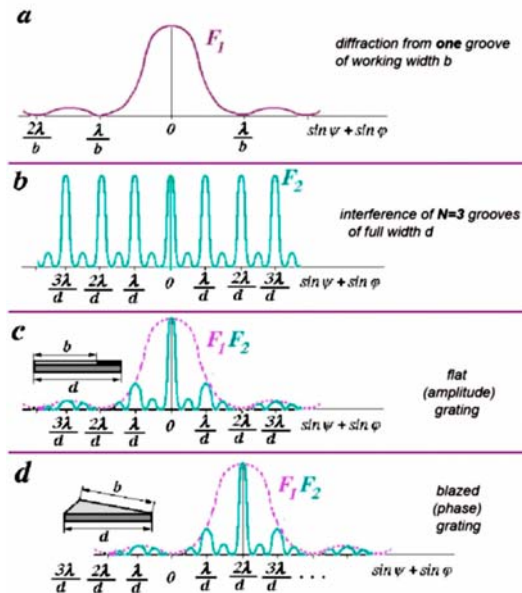


Figure 10. Intensity distribution after interference of the beams in a diffraction grating

The question of what image the grating produces in the zero-order is of particular interest. Then *the grating works simply as flat mirror*, superposing all wavelengths in one direction. We also can consider every flat mirror as a grating with infinite density (or zero constant, $d=0$). Then the only working order will be $k_{max} = 0$. Unfortunately, just in the zero order the maximum energy is concentrated (Fig. 11).

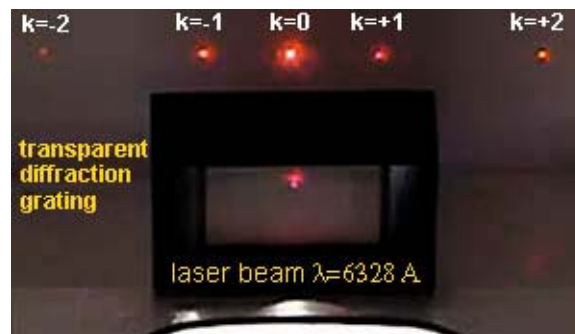


Figure 11. Spectral orders of laser light ($\lambda = 6328\text{\AA}$) passing through a transparent 1200 mm^{-1} diffraction grating

It is necessary to put additional phase-difference to concentrate the intensity-maximum in other than zero order. This is achieved by profiling the grooves' shape in the "blazed" gratings (also called "phase gratings") – Fig. 9b. The additional phase difference in the optical path is equal to $2h/\lambda$ where $h = d \sin \alpha$ is the groove depth and α is the blaze angle.

Example: if the the grating Baush&Lomb, 632 mm^{-1} , $\alpha = 14.7^\circ$ from the grating set in NAO was not phase one, (i.e., if $\alpha = 0$), the limiting order for $\lambda = 6500\text{\AA}$ must be $k_{max} = 4.86$, i.e., 4th. For a grooves' slope of $\sim 15^\circ$ we have $\sin \alpha = 0.25$ and hence for this wavelength the grating will have a maximum in the 1st order.

2.4.3. Free spectral interval

The free spectral range of a diffraction grating is defined as *the largest bandwidth $\Delta\lambda$ in a given order, which does not overlap the same bandwidth in a neighbour order.*

If $\lambda_1 < \lambda_2$ are the extremes of the spectrum band then overlapping will occur at the long wavelength end of the spectrum when λ_2 in order k is diffracted at the same angle as in order $k+1$. Conversely, overlapping will occur at the short wavelength end when λ_1 in order k coincides with λ_2 of order $k-1$. The required conditions to avoid overlapping, is:

$$\Delta\lambda = \lambda_2 - \lambda_1 \geq \lambda_1/k \quad \text{or} \quad \Delta\lambda = \lambda_2 - \lambda_1 \geq \lambda_2/(k-1).$$

Since $\lambda_1 < \lambda_2$, we may say that the free spectral range is equal to the shortest wavelength in the allowed bandwidth divided by the order number.

2.4.4. Angular magnification of the grating. Angular and linear dispersion

It follows from the grating equation that for given λ certain increase in the incident angle correspond to strictly definite increasing of the diffraction angle, i.e., the angular magnification g is simply the derivative $d\varphi/d\psi$. Differentiating the grating equation by constant λ we obtain

$$g = d\varphi/d\psi = \cos\varphi/\cos\psi.$$

Obviously, for the zero order ($\varphi = -\psi$) and for the auto-collimation scheme when the angles of incident and diffraction are equal, $g = 1$.

The derivative by λ gives the *angular dispersion* $d\varphi/d\lambda$ of the grating in order k for given incident angle:

$$d\varphi/d\lambda = k/(d\cos\varphi).$$

As can be seen, for small angles φ , i.e., for low spectral orders, the dependence of the dispersion of DG from the diffraction angle φ is quite weak as far as the change of φ in these orders is in narrow range (0.1 – 0.2 rad). Conversely, the dispersion of the prism is caused by the variable *refractive coefficient* n (according to the Hartman-formula it depends on wavelength as λ^{-2}) and is strongly irregular and inconvenient in work. From the above formula one can conclude that, observing the spectrum along the grating's normal (called "normal" spectrum) the dispersion remains constant and equal to $k/(d\cos\varphi) = k/d$.

Example: let's consider the grating Baush&Lomb, 632 mm^{-1} , $\alpha = 14.7^\circ$ in 1st order. The grating constant is $d = 1.58 \mu$ and the angular dispersion (with accuracy to $\cos\varphi$) will be $1/1.58 = 0.63 \text{ rad}/\mu = 0.000063 \text{ rad}/\text{\AA} = 36^\circ/\mu$ or $36^\circ * 3600''/10000\text{\AA} = 13''/\text{\AA}$.

The angular dispersion determines the *linear dispersion* $dl/d\lambda$ in the focal plane of the spectrograph's camera:

$$dl/d\lambda = F_{cam}(d\varphi/d\lambda).$$

More often the *reverse linear dispersion* D_λ is used:

$$D_\lambda = d\lambda/dl = 1/F_{cam}(d\varphi/d\lambda).$$

Example: for the grating from the above example when the spectrum is registered in the 3rd camera with $F_{cam} = 1900 \text{ mm}$ ($1.9 * 10^6$) the realised reverse linear dispersion will be: $D_\lambda \approx 1/(1.9 * 10^6 \mu * 0.000063 \text{ rad}) \approx 1/120 \text{ \AA}/\mu = 1/120/1000 \approx 8.4 \text{ \AA}/\text{mm}$.

2.4.5. Spectral lines curvature

Due to the finite size of the slit height the rays far from the optical axis fall to the main grating plane under small angle β . The grating equation for these rays will be written as $(\sin\psi + \sin\varphi) = k\lambda/d\cos\beta$. It is equivalent

to shorten the grating constant as $d\cos\beta$. In a result, for the inclined rays the diffraction angle is somewhat greater, the angular dispersion too and the image of the straight entrance slit has a curvature on the focal plane of the camera. For the diffraction grating *the endmost points are displaced in longward side of the wavelength scale* (contrary to the case of prism!). The shape of the spectral lines due to this effect is almost parabolic with a radius of curvature ρ in the centre

$$\rho = dF_{cam}\cos\varphi/k\lambda = F_{cam}\cos\varphi/(\sin\psi + \sin\varphi).$$

This effect increases with the spectral order and with the wavelength!

Example: the full height of the slit of the coude at Rozhen is 10 mm. Working with the big collimator $F_{coll}=10800$ mm we have angle β of only 0.025° or $1.5'$ and the effect is negligible ($\cos 0.025^\circ=0.9999996$). The displacement of the line-ends is only a few microns, much smaller than the pixel size (24μ). But for echelle-spectrometers working in high spectral orders ($k=30 - 100$) this effect is of importance. Also the effect must be considered when the comparison line spectrum was registered.

2.5. Energy distribution in the diffraction grating. Maximum of concentration

As it was shown the picture given by the DG is a result of two processes: *diffraction* from a single element and *interference* of all N beams in given direction. Let's consider a ruled grating with blaze angle α . Two conditions must be performed simultaneously in order to achieve maximum energy concentration: a)- every single element (groove) must reflect in zero order (when the angles of incidence and diffraction are equal in modulus) in direction of the main diffraction maximum for the whole grating; b)- the zero order for the whole grating to be in the direction of the minimum for the single groove. It is clear that the normals to the grating plane and to the single groove differ by angle α . For such a geometry it can be shown that the relation

$$2 \cos(\psi-\alpha) \sin\alpha = k\lambda/d$$

is fulfilled. This relation allows to calculate the blaze angle α if we know the incident angle ψ , the wavelength λ and the spectral order k .

Another important relation connects the blaze angle α and the working width b of the groove: $\sin(\psi+\alpha) - \sin(\psi-\alpha) = 2\sin\alpha\cos\psi = \lambda/b$. According to the values of these quantities the cutter for ruling the grating is sharpened.

It can be shown that for such "phase"-grating the following expression is true:

$$\varphi = 2\alpha - \psi.$$

So the angle of diffraction when the intensity will be maximum is defined. For the autocollimation scheme, when $\varphi = \psi = \alpha$, we obtain for the wavelength of the maximum reflectance the relation:

$$k\lambda_{max} = 2d\sin\alpha.$$

Example: In Fig. 12 the dependence of the wavelength $\lambda_{max} = (2d\sin\alpha)/k$ for different orders for gratings with density 632 l/mm (such as the Baush&Lomb gratings of the NAO' set) in *autocollimation*. So for our grating with $\alpha=14.7^\circ$ we read $\lambda_{max}(1^{st} \text{ order}) \approx 8000 \text{ \AA}$ and for the grating with $\alpha=22.3^\circ$ - a value $\approx 12000 \text{ \AA}$ for the 1st order. One can note also from the same figure that the 14.7° -grating can be used only in the 1st and 2nd orders because the 3rd one lies in the near UV region stopped by the earth atmosphere, while the second grating can successfully work in 3rd order too. As it will be shown below these relations are displaced in the spectrographs working *out of autocollimation mode!*

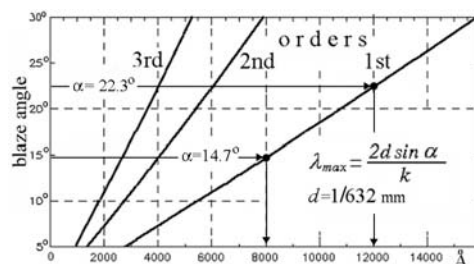


Figure 12. Dependence of the wavelength of maximum reflection λ_{max} in auto-collimation on the blaze angle for different spectral orders for gratings with groove density of 632 lines/mm. The values of λ_{max} for the 1st order are denoted for two gratings.

The above cited relations are obtained for auto-collimation scheme when the angles of incidence and the diffraction are equal (towards the grating's plane) and the diffracted ray goes back to the collimator which can play a role of *camera* mirror! The real coude-spectrographs more often are designed so, that the axes from the grating to the collimator and to the camera make certain angle γ (see Fig. 5). For example, for our coude this angle is $\gamma=41^\circ 45'$ for the big collimator and 43° for the small one. In the case $\gamma \neq 0$ and λ_a as the wavelength in auto-collimation, the wavelength of the maximum reflection are transformed to

$$\lambda_{max} = \lambda_a \cos(\gamma/2).$$

The displacement can be significant. So, for the grating B&L, 632/14.7° in 1st order we have $\lambda_a = 8030 \text{ \AA}$ while in our spectrograph with the big collimator $\lambda_{max} = 7503 \text{ \AA}$. If this grating works with the small collimator ($D=200 \text{ mm}$) than $\gamma=43^\circ$. Then the displacement will differ by 32 \AA for 1st order and by 16 \AA for 2nd one from that for the big ($D=300 \text{ mm}$) collimator.

In Fig. 13 the theoretical distribution of the reflection by "our" grating B&L, 632/14.7° is compared with the measured directly for other B&L grating with blaze angle 14.65° .

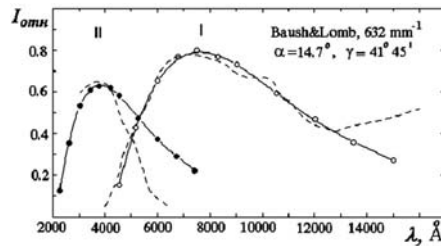


Figure 13. Calculated distribution of the reflection for a grating with groove density of 632 lines/mm and blaze angle 14.7° working in the coude-spectrograph with collimator $D=300 \text{ mm}$ (dots, circles and solid line) and the really measured curves for grating B&L, 632 mm-1, 14.65° . The measured data were published for auto-collimation mode and re-calculated for $\gamma=41^\circ 45'$.

2.6. Evaluation of the parameters of a stellar coude-spectrograph

Now we are ready to evaluate the needed parameters of a coude-spectrograph like this for the 2-m RCC in Rozhen.

The input parameters are:

1. The focal distance of the coude-focus of the telescope: $F_T=72000 \text{ mm}$ ($D/F_T=1:36$);
2. The scale on the slit in the coude-focus: $1''=0.36 \text{ mm}$ (working slit $s_{1''}=0.36 \text{ mm}$);
3. The dome diameter: $\sim 22 \text{ m}$;
4. Desired reverse linear dispersion in order $k=1$: say, $D_\lambda \approx 10 \text{ \AA/mm}$;
5. Working spectral interval; from $<4000 \text{ \AA}$ till $>10000 \text{ \AA}$;
6. Detector pixel size: $p \approx 0.020 \text{ mm}$ (20μ).

2.6.1. First approximation:

1. Choise of grating: it is known that most accessible on the market are gratings with grooves density $N_1 \sim 600$ or 1200 mm^{-1} (i.e., a constant $d = 0.0017 \text{ mm} = 17000 \text{ \AA}$ or $0.00085 \text{ mm} = 8500 \text{ \AA}$).

2. Such a grating will have angular dispersion $d\varphi/d\lambda \approx k/d$:

$$d\varphi/d\lambda \approx 1/17000 \approx 6 \cdot 10^{-5} \text{ rad/\AA} \text{ (or } 1.2 \cdot 10^{-4} \text{ rad/\AA)};$$

3. Evaluating the dimensions of the camera:

$$F_{cam} = 1/[D_\lambda (d\varphi/d\lambda)] = 1/(10 \cdot 6 \cdot 10^{-5}) = 10^5/60 \approx 1700 \text{ mm};$$

4. Evaluating the dimensions of the collimator:

$$F_{coll} = (s/p) F_{cam} = (0.360/0.020) \cdot 1700 > 20000 \text{ mm} = 20 \text{ meters!}$$

But such great focal distance is unacceptable because:

a) goes out of the dome-dimensions (20 m in diameter);

b) needs a diameter of the collimator (i.e., the size of the grating, too) $D \approx 650 \text{ mm}$ (there is not so big single-piece ruled gratings)!

Compromise: we limited ourself to the focal distance $F_{coll} = 10 \text{ m}$. Of course, this means that we *must* decrease also twice the working width of the slit, not $s=1''$ but with slit of 0.15 mm ($<0.5''$). **So that we must accept the necessity to loss light on the slit!**

As soon as we choose $F_{coll} \approx 10000 \text{ mm}$ then its aperture will be around 300 mm . It is quite appropriate – there exist gratings of such dimensions! Finally we choose a collimator with diameter 300 mm and focal distance $300 \times 36 = 10800 \text{ mm}$ (note that these figures perfectly coincide with the real parameters of our coude!)

5. Evaluating the blaze angle in autocollimation for the mean wavelength of our spectral range $\lambda = 7000 \text{ \AA}$:

$$\text{tg } \alpha = \lambda / (2 F_{cam} D_\lambda) = 7000 / (2 \cdot 1700 \cdot 10) = 7/34 \approx 0.20, \text{ or } \alpha \approx 12^\circ.$$

This is an “ordinary” grating and in the then time (the early 70-es of the 20th century) catalogue of the firm *Bausch&Lomb* (Rochester, NY) we find a suitable offer: a family of phase (blaze) gratings with density of 632 l/mm and blaze angle near 14.7° , size along the groove 200 and 300 mm that works in 1st and 2nd orders.

Finally, we choose a grating *Bausch&Lomb*, $632/14.7^\circ$, $300 \times 360 \text{ mm}$! By the way, its price was $36000\$$!

Now the second approximation begins to precise the device we want to order.

2.6.2. Second approximation:

1. Cameras: for maximum aperture of the beam 300 mm and moderate focal ratio, say $1:7$, we obtain for the biggest camera a focal distance of $F_{cam} \approx 2000 \text{ mm}$ [note that the real camera 3 in coude has $F_{cam} = 1900 \text{ mm}$ ($D:F = 1:6.3$)]. Such a camera must be of Schmidt-type and will provide us a dispersion $D_\lambda = 8.3 \text{ \AA/mm}$ in 1st order. The set of achieved dispersions usually is planned by coefficient of 2. So that it is good if the second camera to give in the same order $D_\lambda \approx 15-16 \text{ \AA/mm}$. It can be achieved by a camera with $F_{cam} = 1000 \text{ mm}$ (the real camera 2 of the spectrograph in NAO has $F_{cam} = 875 \text{ mm}$ and provides a dispersion about 18 \AA/mm).

Following the same logic we can plan a third camera which focal distance could be about 500 mm . But for a beam of 300 mm aperture the focal ratio becomes too high for normal production – $1:1.7$. That is why it must work only with smaller collimator, say, with $D = 200 \text{ mm}$. Then the camera will have $D:F = 1:2.5$ that is easier aim. The real camera in the spectrograph in NAO has $F_{cam} = 450 \text{ mm}$ ($1:2.25$) and needs flatfielding lens just before the focal plane because of great curvature of the initial Schmidt-focal-surface!

2. Collimators: There will be better if our chosen collimator with $D = 300 \text{ mm}$ and $F = 10800 \text{ mm}$ is of «of-axis» type with small angle ($<4-5^\circ$) for easier and cheaper production. The camera considerations and the budget-frames show that we must buy also gratings of size 200 mm . They will work properly with a collimator with $D = 200 \text{ mm}$ (and $F = 200 \times 36 = 7200 \text{ mm}$). Hence we can order a second collimator with the cited parameters.

3. Parameters of the other gratings: for more-short wavelengths (5000 \AA) in the 2nd order ($D_\lambda \approx 4 \text{ \AA/mm}$) will be of necessity a grating with blaze angle:

$$\text{tg } \alpha = \lambda / (2 F_{cam} D_\lambda) = 5000 / (2 \cdot 1900 \cdot 4) = 7/34 \approx 0.33 \text{ or } \alpha \approx 18^\circ.$$

The same B&L catalogue offered a grating $632/22.3^\circ$, $200 \times 300 \text{ mm}$, and the Russian firm GOI (Gosudarstvennyy Opticheskiy Institute=State Optical Institute) from Moscow offers similar grating having density 600 mm^{-1} and blaze angle 28° . It has «bluer» reflection and works in orders 2-4. **We immediately buy both gratings, order the equipment, finish the funding and finally STOP our ruinous enthusiasm!**

Thus our task to evaluate and order a suitable equipment for the 2-m telescope is realized!

3. SPECTROGRAPHS WITH CROSS-DISPERSION (ECHELLE SPECTROGRAPHS)

3.1. Crossing the dispersion

The wish for higher resolving power $R=k.N$ with *small* apertures, i.e., with more compact spectrographs (smaller and cheaper gratings!) has only one solution: *to work in higher spectral orders k!* One must not forget that, because of the relation $|\sin\psi + \sin\phi| < 2$, the maximum order for given λ , where *diffraction exist*, will be $k=2d/\lambda$, i.e., *in order given grating to work at least in the 1st order its grating constant must satisfy the relation: $d > \lambda/2$.*

Example: So, for $\lambda = 0.8\mu$ we have $d=1/2400=0.42 \mu$, and a grating with 1200 l/mm ($d=1/1200=0.83 \mu$) can work until the 2nd order. But a grating with 2400 l/mm CAN NOT SHOW A SPECTRUM AROUND WAVELENGTH 1μ , BECAUSE OF $d=0.42 \mu < 0.5 \mu$! FOR $\lambda > 8500\text{\AA}$ SUCH A GRATING APPEARS AS A MIRROR!!! A grating with 100 l/mm ($d=10 \mu$), works for $\lambda = 1 \mu$ up to order $k=20$, and for $\lambda = 0.5 \mu$ - up to $k=40$. A very “coarse” grating of only 33 l/mm works for the same lambdas in orders from 60 till 120! Such grating somewhat is easier for production (it has more “clear” surface of the grooves and the cutter wears less!). But, in order to avoid the “overshadowing” of the beams in such a great angles of diffraction, it is necessary the grooves itself to have great blaze-angles - up to 79° ! The light-beam also comes from such a great angle-of-incidence (see Fig.15).

From the grating equation $d(\sin\psi + \sin\phi) = k\lambda$ we have $k\lambda = k'\lambda'$ that determines the overlapping of spectra of different orders. We can eliminate the undesirable intervals using *filters, scanning monochromators* or, most radically, by *crossing dispersion*.

Let's write the expression for the reversed linear dispersion D_λ in the form (N_1 is the groove density in mm^{-1}):

$$D_\lambda = d/d\lambda = F_{\text{cam}}(kN_1/\cos\phi) = F_{\text{cam}}/\lambda [(\sin\psi + \sin\phi)/\cos\phi].$$

It is clear that, for limited camera's dimension (F_{cam}), the only way to enhance the linear dispersion is to enlarge the angles of incidence and dispersion. For auto-collimation scheme ($\psi=\phi$) we have

$$\sin\psi = \sin\phi = k\lambda N_1/2.$$

The possibilities here are scarce since the value of N_1 is limited (at least for the ruling gratings) to $\sim 2000 \text{ mm}^{-1}$. So that the possibility to enhance the working spectral order k remains the last choice! But here we meet the strong overlapping of the spectral orders...Remember that, for example, for $\lambda=6000$ and $k=50$ the free spectral range is only 120 \AA . The evidently solution is *to separate in some way the different orders spatially*. This can be achieved by *pre-dispersing* of the white light before it to fall to the “main” disperser. As can be seen in Fig.14, if the directions of light-dispersion are “crossed” we obtain a two-dimensional picture of the spectrum consisting of many “portions” of different spectral intervals.

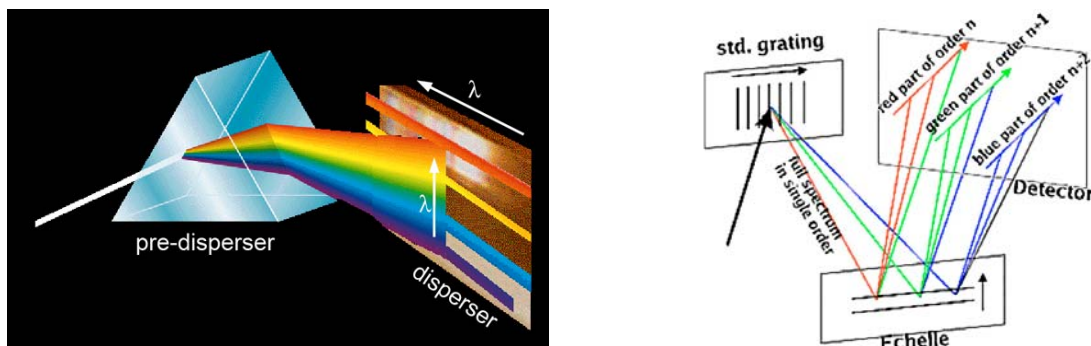


Figure 14. Scheme of crossing dispersions using a prism as a pre-disperser and a grating as a main disperser (at left) and two diffraction gratings (at right).

The pre-disperser (PD) can be a *prism with small refracting angle ($\alpha \sim 10-20^\circ$)* or a *diffraction grating working in 1st order*. Both cases have their characteristics, advantages and disadvantages. The echelle-grating

(Fig.15) has low groove-density (several tens lines-per-mm) and very steep to the gratings-normal reflecting strips.

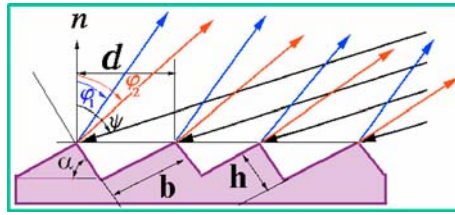


Figure 15. Scheme of echelle grating.

The present echelles have high blaze angle. They usually are called according to the value of their $\text{tg}\alpha$. For example, the gratings produced by the firm *Milton Roy* have $\text{tg}\alpha$ in the interval 2 – 4 (see the table below). The variations of α in the both ends are $<0.4\%$, and of the efficiency - till 2% !

Table: characteristics of the *Milton Roy* echelle-gratings of series “R”

type	α°	D mm	L mm	$N_1 \text{ mm}^{-1}$
R2 ($\text{tg}\alpha=2$)	63.5	390	876	28.2
R2.6	69.0	300	830	29.5
R4	76.0	200	800	30.6

The idea for an echelle-grating was proposed by D. Harrison (MIT and *Bausch&Lomb*) in 1949. The reason was to put an intermediate device for orders-separation between the capabilities of a convenient DG and of *Mickelson's echelon*. The last device has enormous resolving power ($R \sim 1-2\,000\,000$) but is extremely heavy for production.

The most important characteristics of the cross-dispersion scheme are summarized below:

Focal plane geometry (see Fig. 16):

- 1. Linear distance between the orders** - depends on the linear dispersion $dh/d\lambda$ of the pre-disperser (PD) and of the spectral distance $\Delta'\lambda$ produced by the echelle-grating:

$$\Delta'h = \Delta'\lambda (dh/d\lambda).$$

For two adjacent orders k and $k+1$ we have:

$k\lambda = (k+1)(\lambda - \Delta'\lambda) = d(\sin\psi + \sin\phi)$. Hence, for $\Delta'\lambda \ll \lambda$, $\Delta'\lambda = \lambda/(k+1) = \lambda(\lambda - \Delta'\lambda)/d(\sin\psi + \sin\phi) \sim \lambda^2$. Hence $\Delta'h \sim \lambda^2 (dh/d\lambda)$. According to the kind of PD we have:

- PD prism: $dh/d\lambda \sim 1/\lambda^2$ and $\Delta'h \sim \text{const}$
- PD grating: $dh/d\lambda \sim \text{const}$ and $\Delta'h \sim 1/\lambda^2$

2. Slope of the orders - depends on the relation between the linear dispersions of both pre-disperser and the echelle:

$$\text{tg}\theta = (dh/d\lambda)/(dl/d\lambda) \quad (\text{see Fig. 16}).$$

According to the kind of PD we have:

- PD prism: $\text{tg}\theta \sim 1/k\lambda^2$
- PD grating: $\text{tg}\theta = N_{11}/k_2 N_{12}$, (N_1 - the number of lines per mm)

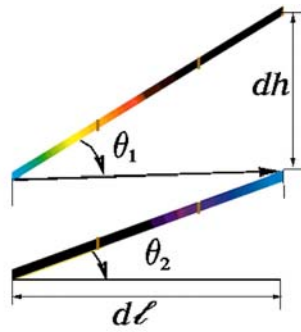


Figure 16. Scheme of echelle orders' slope

The final FoV on the detector in an echelle-spectrograph (see Fig. 17) depends of the kind of PD:

a) **PD prism:** $d\phi/d\lambda \sim dn/d\lambda \sim 1/\lambda^2$: the spectral orders are curved (parabolas), and they are condensed toward the long-wavelength end!

b) **PD grating:** $d\phi/d\lambda \sim \text{const}$: the orders are straight lines with different slope, and they are condensed toward the short-wavelength end!

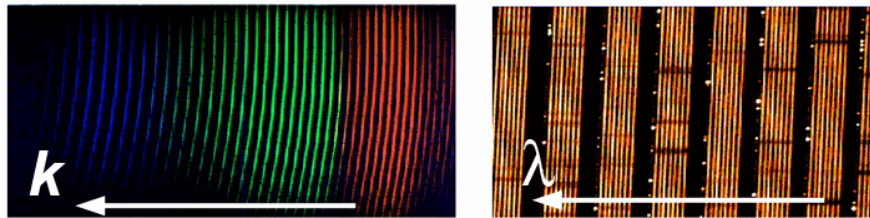


Figure 17. Focal plane geometry in echelle-spectrographs with prism (at left) and grating (at right) pre-disperser.

The principle design and the physical view and dimensions of an echelle astro-spectrograph are presented in the Fig.18. The device is mounted on a thick polished granite plate and has a thermic insulated hood. The approximate size of the granite table is about 1x1 m².

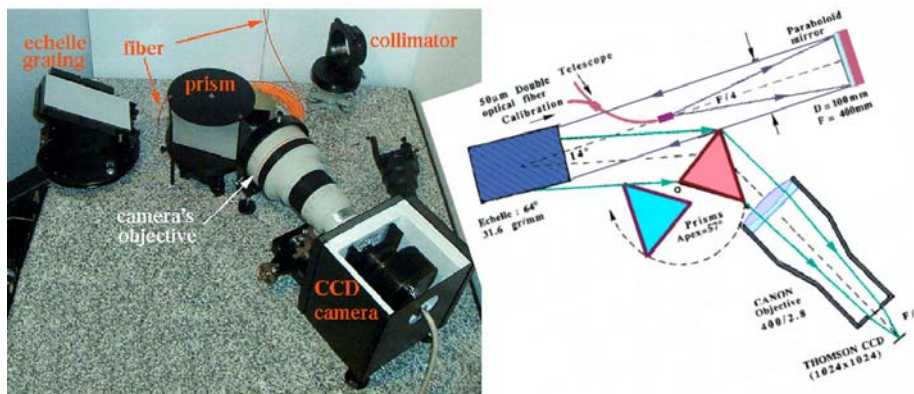


Figure 18. General view (cover removed) and a scheme of the MUSICOS-type echelle spectrograph of Poznan University, Poland.

3.2. Echelle-spectrograph UVES (VLT)

As an example in Fig. 19 we present the VLT-echelle spectrograph UVES – UV-Visual-Echelle-Spectrograph (operating since 2003 in the Nesmyth-focus of UT2-KUEYEN).

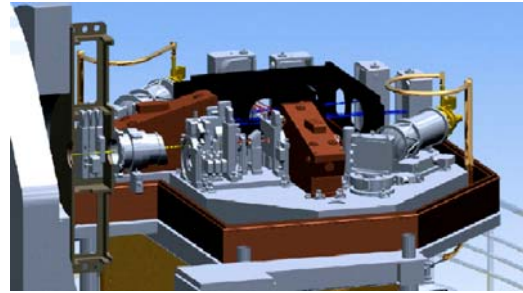
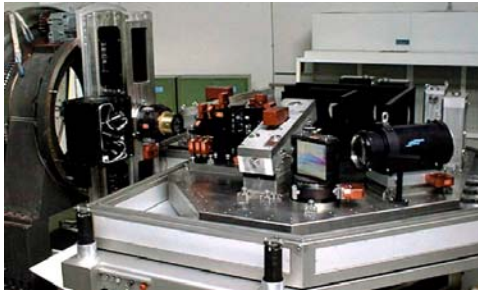


Figure 19. General view (cover removed) and a 3D-scheme of UVES.

UVES has 8 fibers: 2 “sky” and 6 “objects”. With a 1"-fibers this allows multi-object spectroscopy with $R = 40000$ in the region 4200 - 11000 Å. The spectrograph works in two “arms” – blue and red and its characteristics are given in the table below:

	Blue arm	Red arm
Wavelength range	3000 - 5000 Å	4200 - 11000 Å
Resolution-slit product	41400	38700
Max. resolution	~80000 (slit 0.4")	~110 000 (slit 0.3")
Limiting magnitude (1.5hr, S/N~10, slit 0.7")	18.0 at $R = 58000$	19.5 at $R = 62000$
Overall DQE	12 % at 4000 Å	14 % at 6000 Å
Dioptric cameras	F/1.8, 70 $\mu\text{m}''$, field 43.5 mm	F/2.5, 97 $\mu\text{m}''$, field 87 mm
CCDs and pixels	EEV 2K x 4K, 15 μm pix (0.22 "/pix)	mosaic (EEV + MIT/LL), 2Kx4K, 15 μm pix (0.16 "/pix)
Crossdispersers (g/mm and wavelength of max. efficiency)	#1: 1000 g/mm 3600 Å #2: 660 g/mm 4600 Å	#3: 600 g/mm 5600 Å #4: 312 g/mm 7700 Å
Typical wavelength range/frame CD#1(#2) and CD#3(#4)	850 (1260) Å in 33 (31) orders	2000 (4030) Å in 37 (33) orders
Order separation (min')	10" or 40 pixels	12" or 70 pixels

Each of the “blue” and “red” echelle-gratings for this spectrograph is a mosaic of two single gratings with characteristics given in the next table. Note the big length of the mosaics needed to match the long elliptic shape of the cross-section of the falling to the grating collimated beam. Note also the huge difference between the theoretical resolving power ($\sim 2 \cdot 10^6$) and the working one ($\sim 10^5$)! This gives a good example for the compromises that the astro-spectroscopists are forced to make in order to reach weaker limit magnitude. The peak DQE of the CCDs for UVES reach 90% and in the ends of the working spectral intervals the efficiency is not less than 50% in UV and is $\sim 20\%$ in the near IR. The first stellar spectra with UVES were obtained in the late 2002 (Fig.20).

	<i>Blue echelle mosaic</i>	<i>Red echelle mosaic</i>
Dimensions	840x214x125 mm	840x214x125 mm
Groove density	41.6 g/mm	31.6 g/mm
Blaze angle	76.0°	75.07°
Absolute efficiency at the order center	65% at 3500 Å	71% at 5500 Å
Max resolution (diffraction limit)	1 900 000 (!) (0.033 Å at 6328 Å)	2 100 000 (!!) (0.030 Å at 6328 Å)
Nominal resolution (0.5 arcsec slit)	82 000	77 400
Spatial resolution	0.1" on the sky	0.09" on the sky
Ghosts; satellites	$< 5 \times 10^{-5}$	$< 8 \times 10^{-5}$

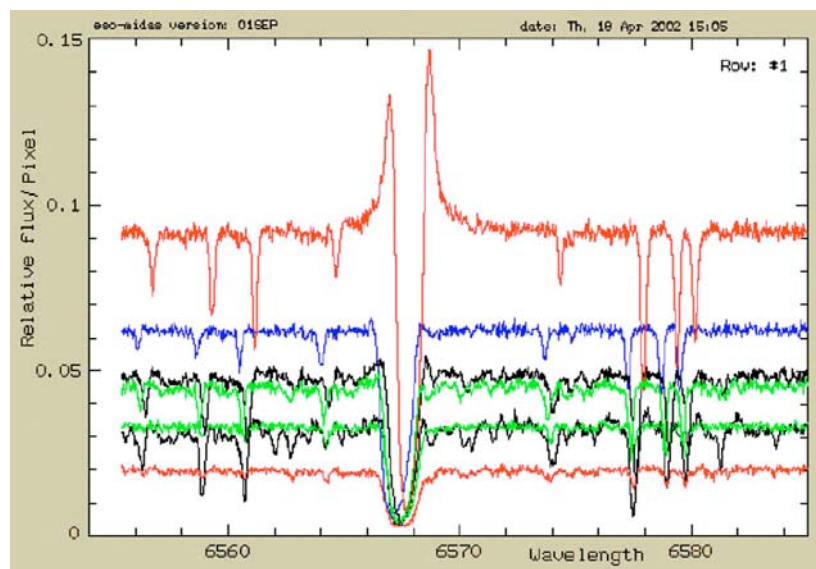


Figure 20. A set of test-spectrograms obtained with UVES.

4. NEW TENDENCIES IN ASTRO-SPECTROSCOPY

4.1. Multi-object spectroscopy

The mid-20th century tendency to build *universal* big telescopes now is abandoned. Now almost all big projects for astronomical equipment are concentrated on the designing a specialized instrumentation. According to the spectral observations the most advanced technique usually includes multi-object capabilities (tens and even hundreds channels). The next generation wide-field instrumentation will grow the number of simultaneously registered star-channels from the present ~500 to 4000-5000! As an example the projects KAOS (Kilo Aperture Optical Spectrograph) for 8-m Gemini, WFMOS (Wide Field Multi-Object Spectrograph) for 8.3-m Subaru or MUSE for VLT can be noted. These facilities will include a set of tens identical spectrographs feeding each by tens or even hundred object-fibers.

4.2. 3-D spectroscopy

The next important tendency is called “3-D” or Integral-Field-Spectroscopy. Here the idea is to obtain a spectrum from every “elementary element” of the 2-D field in the telescope’ focus. In fact so called “data

cube” is obtained. Using such a technique one can easily obtain, for example, the radial velocity “map” of the whole FoV of the telescope!

5. OPTIMISTIC CONCLUSIONS

The new instrumentation will increase drastically the information-flow from the telescopes and will need new methods for processing and maintenance of the data. An element of the new organizing of our science is the Virtual Observatory, giving an access to enormous data bases for multi-national astronomical community.

Placing adequate spectral equipment on earth orbit or even on the Moon, it will be possible to work with greater resolving power and with greater efficiency than by the ground-based telescopes. The much greater expenditures for such instrumentation will be, of course, easily justifiable by the value of the new astrophysical data that surely will be obtained!